# The Ca$^{2+}$/Mn$^{2+}$ ion-pump PMR1 links elevation of cytosolic Ca$^{2+}$ levels to α-synuclein toxicity in Parkinson's disease models

S Büttner[1,12], L Faes[2,3,12], WN Reichelt[1,12], F Broeskamp[1], L Habernig[1], S Benke[1], N Kourtis[4], D Ruli[1], D Carmona-Gutierrez[1], T Eisenberg[1], P D'hooge[2], R Ghillebert[3], V Franssens[3], A Harger[5], TR Pieber[5], P Freudenberger[1], G Kroemer[6,7,8,9,10], SJ Sigrist[11], J Winderickx[3], G Callewaert*,[2], N Tavernarakis[4] and F Madeo*,[1]

Parkinson's disease (PD) is characterized by the progressive loss of dopaminergic neurons, which arises from a yet elusive concurrence between genetic and environmental factors. The protein α-synuclein (αSyn), the principle toxic effector in PD, has been shown to interfere with neuronal Ca$^{2+}$ fluxes, arguing for an involvement of deregulated Ca$^{2+}$ homeostasis in this neuronal demise. Here, we identify the Golgi-resident Ca$^{2+}$/Mn$^{2+}$ ATPase PMR1 (plasma membrane-related Ca$^{2+}$-ATPase 1) as a phylogenetically conserved mediator of αSyn-driven changes in Ca$^{2+}$ homeostasis and cytotoxicity. Expression of αSyn in yeast resulted in elevated cytosolic Ca$^{2+}$ levels and increased cell death, both of which could be inhibited by deletion of PMR1. Accordingly, absence of PMR1 prevented αSyn-induced loss of dopaminergic neurons in nematodes and flies. In addition, αSyn failed to compromise locomotion and survival of flies when PMR1 was absent. In conclusion, the αSyn-driven rise of cytosolic Ca$^{2+}$ levels is pivotal for its cytotoxicity and requires PMR1.

*Cell Death and Differentiation* (2013) **20**, 465–477; doi:10.1038/cdd.2012.142; published online 16 November 2012

α-Synuclein (αSyn) is a small, natively unfolded protein that is abundantly expressed in the central nervous system. It constitutes the major structural component of the intracellular protein inclusions termed Lewy bodies that define a pathological hallmark of Parkinson's disease (PD).[1] Mutations in or duplication and triplication of the gene coding for αSyn all result in familial PD.[2–6] An increasing body of evidence points towards a role for Ca$^{2+}$ ions and Ca$^{2+}$-dependent processes in the pathology of PD in general[7,8] and αSyn-mediated neuronal death during PD in particular.[9–12] The underlying mechanisms, however, remain enigmatic. A valuable tool to explore such pending questions are humanized yeast models based on heterologous expression of human αSyn and pathogenic mutants, as they have not only recapitulated several features of PD but have also allowed to identify novel and evolutionary-conserved mediators and processes involved in the cytocidal consequences of αSyn.[13–17] As the regulation of Ca$^{2+}$ homeostasis is highly conserved between yeast and mammals – with the advantage of reduced complexity and redundancy in

yeast[18–20] – we heterologously expressed human αSyn in yeast to elucidate its effect on Ca$^{2+}$ homeostasis and cell death. We could identify the Golgi-resident Ca$^{2+}$/Mn$^{2+}$ ATPase PMR1 (plasma membrane-related Ca$^{2+}$-ATPase 1) as mediator of αSyn-driven changes in Ca$^{2+}$ homeostasis and cytotoxicity in yeast, nematodes and flies.

## Results

**Heterologous expression of αSyn in yeast disrupts Ca$^{2+}$ homeostasis.** We first quantified the basal cytosolic Ca$^{2+}$ levels in yeast cells equipped with the Ca$^{2+}$-dependent reporter protein aequorin at standard external [Ca$^{2+}$] of ∼1 mM in the culture medium. In this setting, heterologous expression of αSyn provoked an elevation of the cytosolic Ca$^{2+}$-concentration, [Ca$^{2+}$]$_{cyt}$, within the first 24 h of expression that subsided after 2 days of culturing (Figure 1a). Simultaneous determination of oxidative stress based on the superoxide-driven conversion of dihydroethidium to
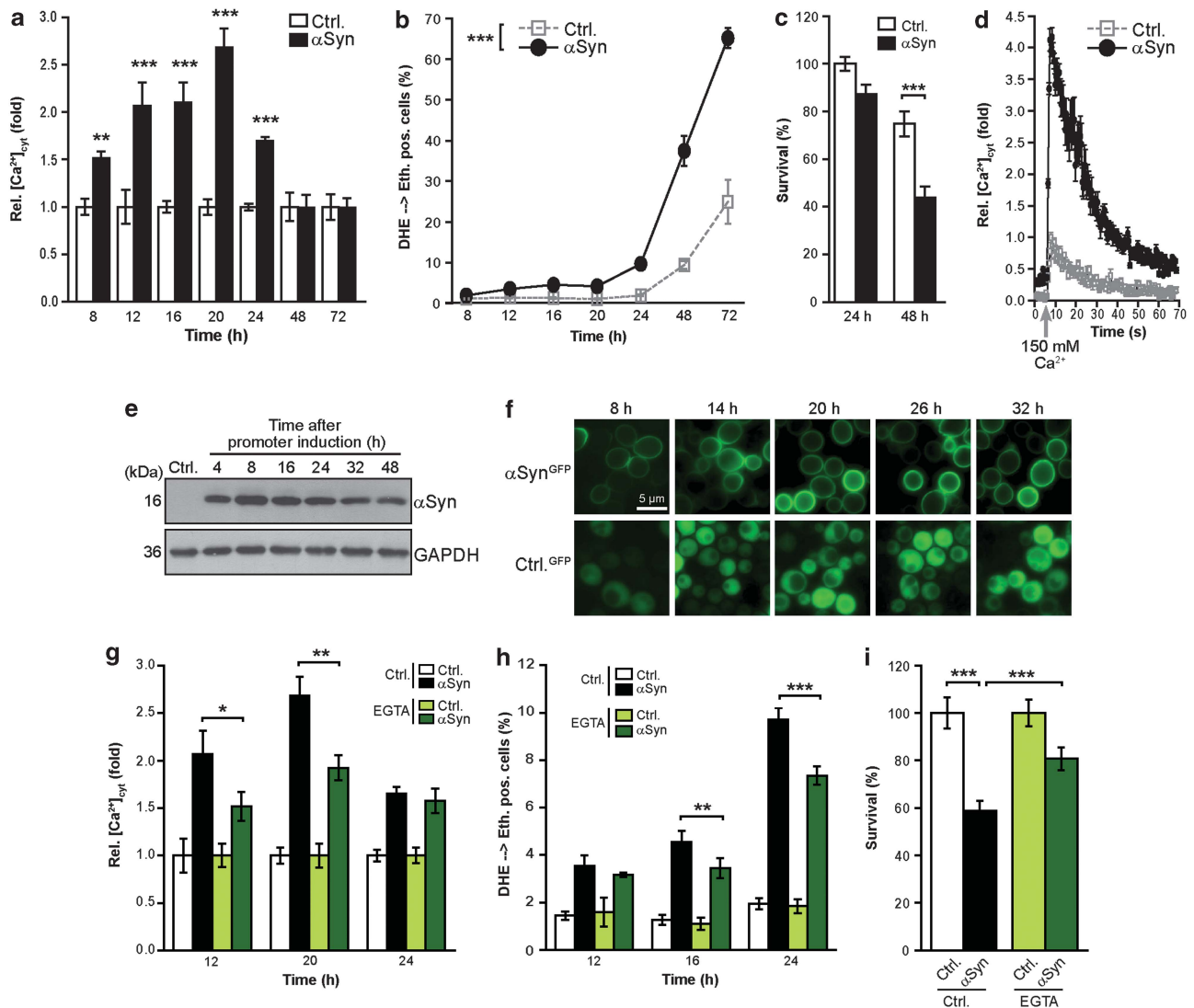
**Figure 1** Heterologous expression of αSyn elevates basal $[Ca^{2+}]_{cyt}$ and amplifies transient $[Ca^{2+}]_{cyt}$ responses in yeast. (**a**) Determination of basal cytosolic $Ca^{2+}$ levels using aequorin-based luminescence measurement of WT yeast cells expressing human αSyn for indicated time or harbouring the empty vector (Ctrl.). Mean ± S.E.M., $n = 8$; ***$P < 0.001$ and **$P < 0.01$. (**b**) Flow cytometric quantification of oxidative stress indicated by the superoxide-driven conversion of non-fluorescent dihydroethidium to fluorescent ethidium (DHE→Eth.) of WT yeast cells expressing human αSyn for indicated time or harbouring the empty vector (Ctrl.). Mean ± S.E.M., $n = 8$; ***$P < 0.001$. (**c**) Survival determined by clonogenicity of WT yeast cells expressing human αSyn or harbouring the empty vector control for 24 h and 48 h. Cells were plated on YEPD agar plates. Mean ± S.E.M., $n = 10$; ***$P < 0.001$. (**d**) Aequorin-equipped yeast cells harbouring the vector control or expressing αSyn for 16 h were challenged with 150 mM $CaCl_2$ and transient $[Ca^{2+}]_{cyt}$ responses were observed for 70 s. Data was normalized to maximum peak amplitude of control cells. Mean ± S.E.M., $n = 6$. (**e**) Western blot analysis of αSyn expression in WT cells. Cells were harvested at indicated time points after induction of galactose-driven expression. Blots were probed with antibodies directed against FLAG-epitope to detect FLAG-tagged αSyn and against glyceraldehyd-3-phosphate dehydrogenase (GAPDH) as loading control. (**f**) Fluorescence microscopic analysis of WT cells expressing GFP-tagged αSyn (αSyn^GFP) or harbouring the corresponding vector control (Ctrl.^GFP) at indicated time points. (**g**) Determination of basal cytosolic $Ca^{2+}$ levels using aequorin-based luminescence measurement of yeast cells expressing human αSyn or harbouring the empty vector (Ctrl.) after growth for 12 h, 20 h or 24 h on galactose media (promoter induction) supplemented or not with 2 mM ethylene glycol tetraacetic acid (EGTA). Data has been normalized to equally treated vector control cells. Mean ± S.E.M., $n = 6$; **$P < 0.01$ and *$P < 0.05$. (**h**) Flow cytometric quantification of oxidative stress by assessing the ROS-driven conversion of dihydroethidium to ethidium (DHE→Eth) upon expression of αSyn for indicated time and supplementation of media with 2 mM EGTA. Mean ± S.E.M., $n = 4$–8; ***$P < 0.001$ and **$P < 0.01$. (**i**) Survival determined by clonogenicity of yeast cells expressing αSyn or harbouring the empty vector control for 48 h and supplementation of galactose medium with 2 mM EGTA. Cells were plated on YEPD agar plates. Mean ± S.E.M., $n = 12$; ***$P < 0.001$

fluorescent ethidium (DHE→Eth) demonstrated that the rise in $[Ca^{2+}]_{cyt}$ triggered by αSyn (Figure 1a) coincided with an increase in oxidative stress. However, the $[Ca^{2+}]_{cyt}$ boost developed well before the massive production of reactive oxygen species (ROS), which started after 24 h of αSyn expression (Figure 1b), and subsequent cell death (Figure 1c). This points towards a sequential course of

events, where αSyn-directed $[Ca^{2+}]_{cyt}$ increase occurs upstream of ROS generation and death. Immunoblot analysis revealed that αSyn (driven by a galactose-promoter) was well expressed throughout the experiment, accumulating around 8 h after promoter induction (Figure 1e). The transient, αSyn-induced increase in $[Ca^{2+}]_{cyt}$ was not related to a different localization of the protein itself, as – in line with

previous studies[15] – green fluorescent protein (GFP)-tagged αSyn was prominently detectable at the plasma membrane within the first 2 days of expression (Figure 1f).

In addition to the disturbance in basal $[Ca^{2+}]_{cyt}$, αSyn altered the cellular response to high extracellular $Ca^{2+}$ pulses. Upon challenge with 150 mM $Ca^{2+}$, a rapid and transient increase in $[Ca^{2+}]_{cyt}$ was detectable that was largely amplified upon expression of αSyn (Figure 1d).

Addition of 2 mM ethylene glycol tetraacetic acid (a $Ca^{2+}$ chelator) to the culture medium partly inhibited the increase in basal $[Ca^{2+}]_{cyt}$ and at the same time ameliorated αSyn-induced accumulation of ROS and cell death (Figures 1g–i). Similar results were obtained using another $Ca^{2+}$ chelator, BAPTA-AM (1,2-bis-(o-Aminophenoxy)-ethane-N,N,N',N'-tetraacetic acid, tetraacetoxymethyl ester), which is cell-permeable and acts as intracellular $Ca^{2+}$ sponge (Supplementary Figures S1A and B). Thus, inhibition of the rise in basal $[Ca^{2+}]_{cyt}$ attenuates subsequent ROS accumulation and death, indicating a causal link between disturbances in $Ca^{2+}$ homeostasis and αSyn-inflicted cellular demise.

Oxidative stress and concomitant oxidation of DNA, proteins and lipids are essentially involved in neuronal cell death in various models of PD.[21–23] Therefore, we tested whether the thiolic antioxidant N-acetylcysteine (NAC), a precursor of glutathione that has been shown to be protective in several PD-associated neurodegenerative scenarios,[24–27] could block αSyn-induced generation of ROS and eventual cell death. Although supplementation with NAC did not prevent the first increase in ROS generation detectable within 24 h, it clearly inhibited massive ROS production and subsequent cell death occurring after 2 days of αSyn expression (Figures 2a–c). Basal $[Ca^{2+}]_{cyt}$ levels were largely unaffected by the addition of NAC (Figure 2d). By contrast, overexpression of cytosolic or mitochondrial superoxide dismutase (Sod1p or Sod2p, respectively) had no effect on αSyn-induced oxidative stress (Supplementary Figures S2A and B), arguing in favour of a rather broad pattern of cellular oxidative stress (that cannot by antagonized by overexpression of superoxid dismutases) as a cause of αSyn-induced cell death.
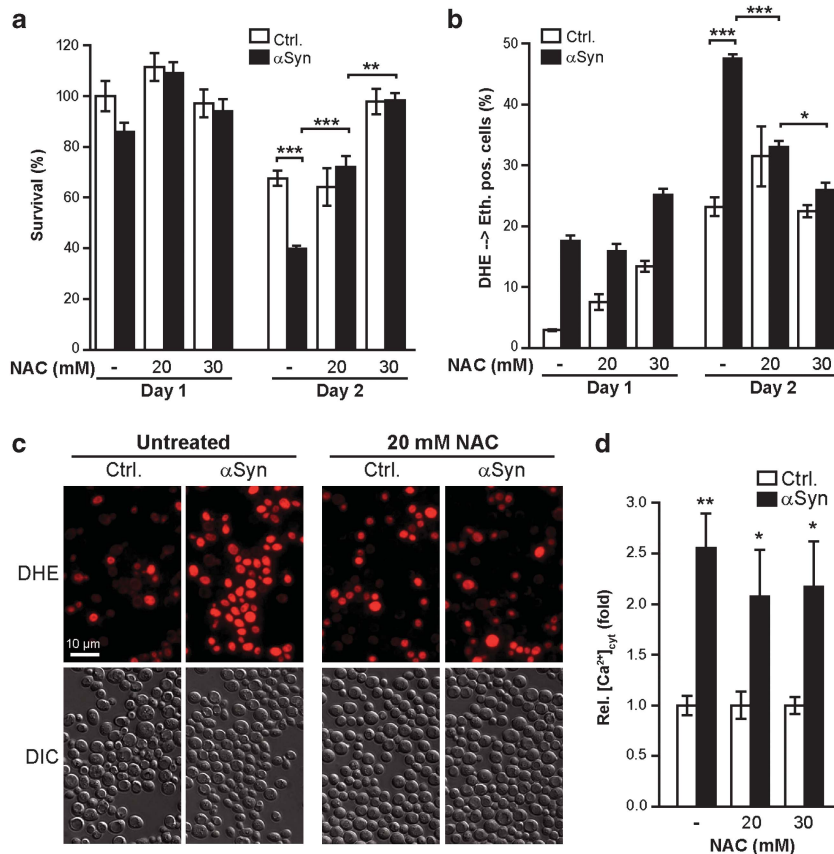


Figure 2 The antioxidant NAC inhibits αSyn cytotoxicity. (a) Survival determined by clonogenicity of yeast cells expressing αSyn or harbouring the empty vector. Galactose growth medium (for promoter induction) has been supplemented or not with 20 mM or 30 mM NAC as indicated and cells were plated on YEPD agar plates at day 1 and day 2 to determine survival. Mean ± S.E.M., $n = 12–18$. Significances have been calculated for day 2, with ***$P < 0.001$ and **$P < 0.01$. (b) Flow cytometric quantification of oxidative stress by assessing the ROS-driven conversion of dihydroethidium to ethidium (DHE → Eth) of cells described in (a). Mean ± S.E.M., $n = 8$. Significances have been calculated for day 2, with ***$P < 0.001$ and *$P < 0.05$. (c) Representative micrographs of dihydroethidium to ethidium (DHE → Eth) staining of cells expressing αSyn or harbouring the empty vector after supplementation of galactose growth medium with 20 mM NAC for 2 days as flow cytometrically quantified in (b). (d) Determination of basal cytosolic $Ca^{2+}$ levels using aequorin-based luminescence measurement of yeast cells expressing αSyn or harbouring the empty vector after growth on galactose media supplemented or not with indicated concentrations of NAC for 20 h. Data has been normalized to equally treated vector control cells. Mean ± S.E.M., $n = 8$; **$P < 0.01$ and *$P < 0.05$

**αSyn cytotoxicity in yeast is facilitated by PMR1.** To identify molecular determinants for αSyn toxicity and dysregulation of $Ca^{2+}$ homeostasis, we monitored αSyn-induced consequences in numerous deletion mutants known to influence $Ca^{2+}$ transport or signalling. Yeast codes for various homologues of mammalian $Ca^{2+}$ channels, transporters, sensors and buffers, including the plasma membrane-located voltage-dependent $Ca^{2+}$ channel Cch1p/Mid1p, the secretory pathway and Golgi-resident $Ca^{2+}$-ATPase Pmr1p, the sarcoendoplasmic reticulum $Ca^{2+}$-ATPase Cod1p, the vacuolar $H^+/Ca^{2+}$ exchanger Vcx1p, the plasma membrane $Ca^{2+}$-ATPase Pmc1p, the vacuolar cation channel Yvc1p – a putative homologue of the mammalian transient receptor potential canonical channels – or the general calcium sensor calmodulin as well as calcineurin and calmodulin-dependent kinases.[18–20] Using deletion mutants of these calcium-related regulators and automated quantification of ROS production, we evaluated the contribution of these proteins to αSyn cytotoxicity. This approach identified PMR1 as a mediator of αSyn-triggered ROS production (Figures 3a and b). In addition, the αSyn-driven development of apoptotic and necrotic markers – assessed using AnnexinV/propidium iodide (PI) co-staining, which allows the discrimination between early apoptotic ($AnnV^+$), late apoptotic/secondary necrotic ($AnnV^+/PI^+$) and necrotic ($PI^+$) cells – demonstrated that deletion of *PMR1* completely inhibited αSyn-driven increase in apoptotic and necrotic populations (Figures 3c and d). By contrast, the absence of *CCH1*, *MID1*, *PMC1*, *VCX1*, *YVC1*, or *COD1* did neither alter αSyn-instigated ROS-accumulation nor cell death markers as compared with wild type (WT; Figures 3a–d). Notably, deletion of these genes did not compromise αSyn expression (Figure 3e). Determination of survival using clonogenic survival plating assays showed that the absence of Pmr1p potently inhibited αSyn-induced cell death (Figure 3f). In addition, we generated a conditional *PMR1* mutant by replacement of the promoter region of *PMR1* with a tetO promoter that is active in the absence of doxycycline and prevents gene expression upon addition of $10\,\mu g/ml$ of the chemical.[28] Treatment of cells with doxycycline and thus depletion of Pmr1p largely reduced αSyn-induced ROS production, confirming that Pmr1p is essentially involved in αSyn cytotoxicity (Figures 3g and h).

To test whether αSyn has any effect on the localization and/or expression levels of Pmr1p, we performed fluorescence microscopy as well as immunoblot analyses of yeast cells endogenously expressing a Pmr1p-GFP fusion protein. No obvious effect on Pmr1p protein levels or Golgi localization was apparent (Figures 4a and b). Using reverse transcription quantitative PCR, we could detect a slight upregulation of PMR1 mRNA (normalized to actin mRNA) after 14 h of αSyn expression (Figure 4c).

We next analysed whether the rise in basal $[Ca^{2+}]_{cyt}$ triggered by αSyn is connected to the upregulation of a specific $Ca^{2+}$ influx system that has been shown to be stimulated in scenarios such as the accumulation of misfolded proteins in the endoplasmic reticulum,[29] different defects in vesicular trafficking[30,31] and depletion of $Ca^{2+}$ from the endoplasmic reticulum, for example, upon *PMR1* deficiency.[32,33] In all of these cases, a high rate of $Ca^{2+}$ uptake via upregulation/activation of a high-affinity $Ca^{2+}$ influx system that involves Cch1p and Mid1p is triggered.[34] Resultant elevated basal $[Ca^{2+}]_{cyt}$ levels lead to the activation of $Ca^{2+}$ signalling pathways essential for initiation of compensatory mechanisms and subsequent cell survival.[34]

Using quantitative PCR, we could indeed detect that after 14 h of expression, αSyn significantly amplified CCH1 mRNA levels and slightly upregulated MID1 mRNA (Figure 4d). As shown for PMR1 mRNA levels (Figure 4c), this effect faded after 24 h (Figure 4d). Given these results, we tested whether proteins involved in the calmodulin/calcineurin pathway and thus responsible for cellular $Ca^{2+}$ sensing might alter αSyn-instigated cytotoxicity. Determination of ROS production demonstrated that αSyn toxicity was mostly unaffected by deletion of genes coding for the calcineurin-responsive zinc finger transcription factor Crz1p and the calmodulin-dependent kinases Cmk1p and Cmk2p, while the absence of Cnb1p, the regulatory subunit of calcineurin (and to some extent the absence of Cna2p, one of two isoforms of the catalytic subunit of calcineurin), did aggravate and expedite αSyn-induced oxidative stress (Figure 4e). Thus, an intact and functional $Ca^{2+}$ signalling pathway that essentially involves calcineurin might contribute to a compensatory mechanism that partly counteracts and/or delays the toxic consequences of αSyn expression.

**Pmr1p mediates αSyn-induced dysregulation of $Ca^{2+}$ homeostasis.** Next, we analysed whether the absence of proteins mediating cellular $Ca^{2+}$ transport modified the αSyn-induced raise in cytosolic $Ca^{2+}$ levels. Consistent with a link between αSyn-mediated toxicity and dysregulation of $Ca^{2+}$-homeostasis, expression of αSyn increased basal $[Ca^{2+}]_{cyt}$ in all deletion mutants except in Δ*pmr1* cells (Figure 5a). In line with previous studies,[35] deletion of *PMR1* already caused increased basal $[Ca^{2+}]_{cyt}$ as visible in the baseline recordings in Figure 5b. Furthermore, the absence of Pmr1p largely inhibited αSyn-induced amplification of rapid, transient cytosolic $Ca^{2+}$ peaks upon addition of 150 mM $Ca^{2+}$ (Figure 5b). Although this remained mostly unaffected upon deletion of *MID1*, *PMC1*, *VCX1* and *YVC1*, the absence of *CCH1* or *COD1* elevated the cellular response to external $Ca^{2+}$ pulses *per se* and prevented further peak amplification by αSyn (Supplementary Figures S3A–F). Similar expression levels of aequorin were observed in all mutants (Figure 5c). Moreover, measurement of the transient elevation of $[Ca^{2+}]_{cyt}$ following the addition of glucose to glucose-starved cells demonstrated that again αSyn provoked an increase in $[Ca^{2+}]_{cyt}$ peak amplitude, which was inhibited in Δ*pmr1* cells (Figure 5d) but present in all other deletion mutants tested (Figure 5e). Thus, Pmr1p is crucially involved in the cellular consequences following αSyn expression, including (i) elevation of basal $[Ca^{2+}]_{cyt}$, (ii) deregulation of the rapid cellular response to sudden external glucose or high $Ca^{2+}$ pulses, and (iii) accumulation of ROS and subsequent death.

**$Ca^{2+}$ rather than $Mn^{2+}$ transport activity of Pmr1p contributes to αSyn toxicity.** The primarily Golgi-resident pump Pmr1p not only supplies $Ca^{2+}$ to both the Golgi complex and the endoplasmic reticulum but also constitutes
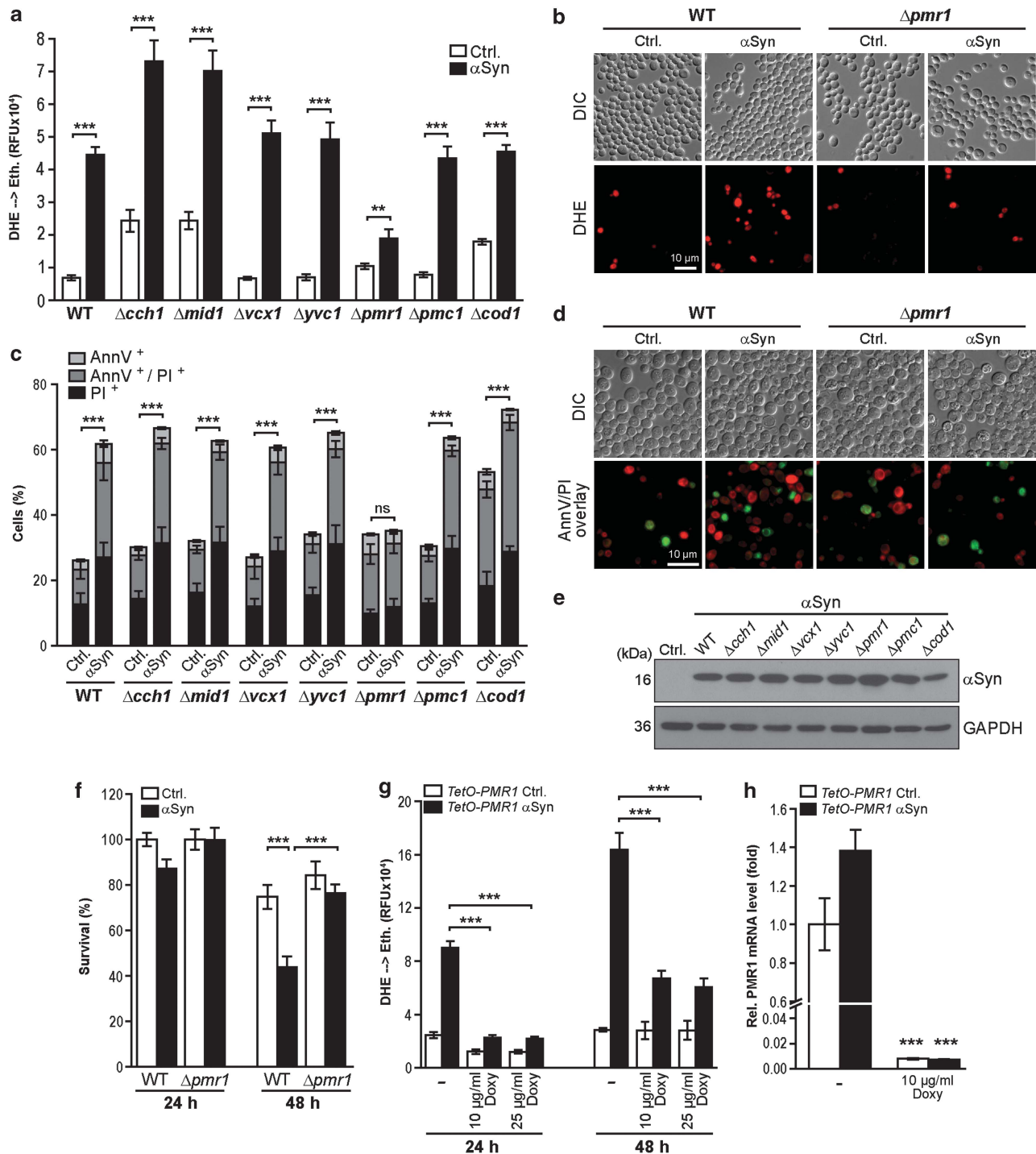
**Figure 3** The Ca$^{2+}$/Mn$^{2+}$ ATPase Pmr1p mediates αSyn cytotoxicity. (**a** and **b**) Quantification via fluorescence reader (**a**) and representative micrographs (**b**) of ROS production by assessing the ROS-driven conversion of dihydroethidium to ethidium (DHE → Eth) upon expression of αSyn for 24 h in WT yeast cells and indicated deletion mutants. Mean ± S.E.M., $n = 8$; ***$P < 0.001$ and **$P < 0.01$. (**c** and **d**) Flow cytometric quantification (**c**) and representative micrographs (**d**) of externalization of phosphatidylserine (AnnV$^+$) and loss of membrane integrity (PI$^+$) by Annexin V/PI co-staining of WT cells and indicated deletion mutants expressing αSyn for 48 h. Mean ± S.E.M., $n = 6$; ***$P < 0.001$. (**e**) Western blot analysis of αSyn expression in WT cells and indicated deletion mutants. Blots were probed with antibodies against FLAG-epitope to detect FLAG-tagged αSyn and against glyceraldehyd-3-phosphate dehydrogenase (GAPDH) as loading control. (**f**) Survival determined by clonogenicity of WT and Δpmr1 yeast cells expressing αSyn or harbouring the vector control after 24 h and 48 h of expression on galactose media and plating on YEPD agar plates. Mean ± S.E.M., $n = 10$; ***$P < 0.001$. (**g**) Quantification of ROS accumulation (DHE → Eth) in yeast cells in which the promoter region of PMR1 has been replaced by a doxycycline-repressible promoter (TetO-PMR1). Doxycycline (Doxy) was added in indicated concentrations and αSyn was expressed for 24 h or 48 h. Mean ± S.E.M., $n = 8$; ***$P < 0.001$. (**h**) Q-PCR-based quantification of PMR1 mRNA levels in yeast cells described in (**g**) after treatment with 10 μg/ml Doxycycline (Doxy) and αSyn expression for 12 h. Data have been normalized to mRNA levels of actin. Means ± S.E.M., $n = 3$. Asterisks indicate significance between untreated and Doxy-treated cells, ***$P < 0.001$
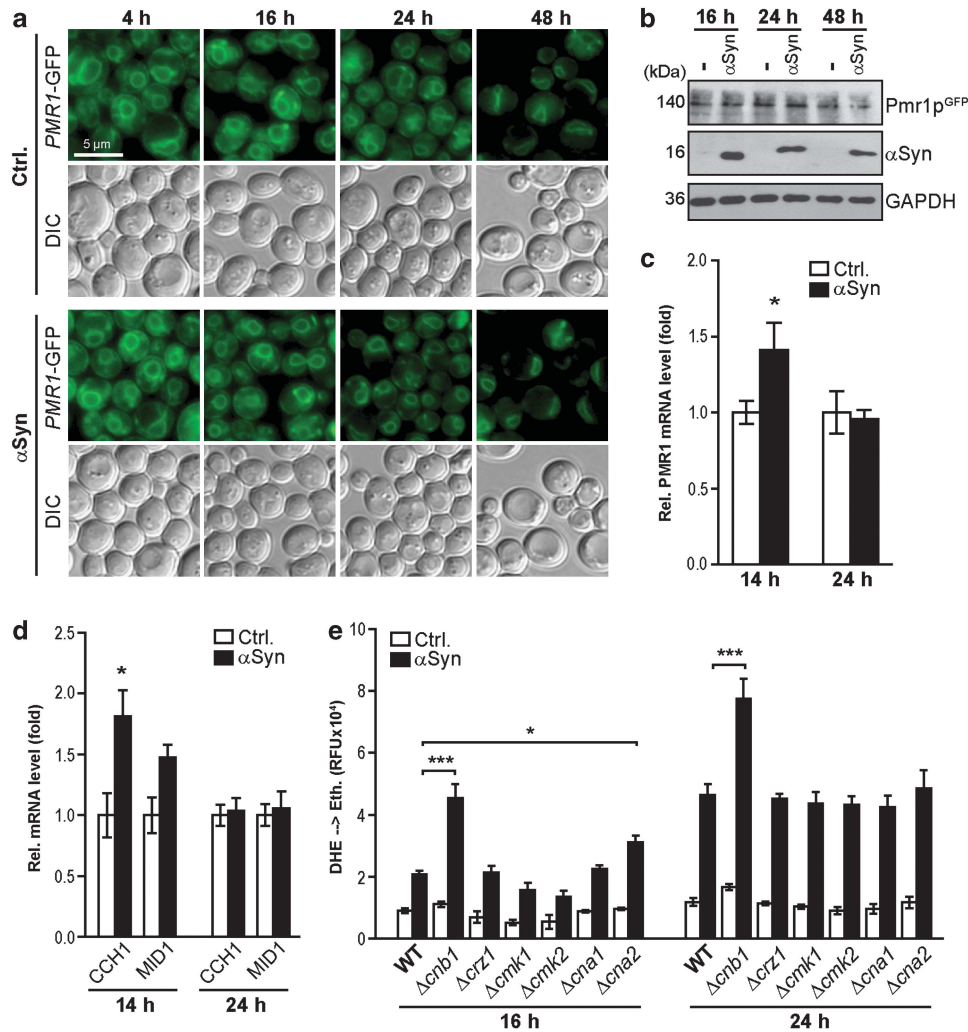
**Figure 4** Expression of αSyn causes a slight upregulation of PMR1 and CCH1 mRNA levels. (**a**) Representative micrographs of yeast cells expressing endogenously GFP-tagged Pmr1p in combination with αSyn or corresponding vector control at indicated time points after induction of αSyn expression. (**b**) Western blot analysis of cells described in (**a**) at indicated time points after induction of αSyn expression. Blots were probed with antibodies against GFP to detect Pmr1p-GFP fusion protein, against FLAG-epitope to detect FLAG-tagged αSyn and against glyceraldehyd-3-phosphate dehydrogenase (GAPDH) as loading control. (**c** and **d**) Q-PCR-based quantification of PMR1 mRNA levels (**c**) and of CCH1 and MID1 mRNA levels (**d**) in WT cells expressing αSyn or harbouring the empty vector control for 14 h or 24 h, respectively, normalized to actin mRNA levels. Means ± S.E.M., $n = 6$–9; *$P < 0.05$. (**e**) Quantification of ROS accumulation (DHE → Eth) in WT yeast cells and indicated deletion mutants expressing αSyn for 16 h or 24 h using a fluorescence reader. Mean ± S.E.M., $n = 6$; ***$P < 0.001$ and *$P < 0.05$

an important route to detoxify excess manganese, providing $Mn^{2+}$ for protein glycosylation in the Golgi complex.[36] Thus, deletion of *PMR1* results in (i) depletion of endoplasmic reticulum $Ca^{2+}$ stores,[33] which in turn causes elevated $[Ca^{2+}]_{cyt}$ via increased $Ca^{2+}$ uptake, as well as in (ii) hypersensitivity to manganese.[36] Defects in cellular manganese homeostasis as well as exposure to manganese have been associated with PD and PD-like syndroms in humans[37,38] and several model systems.[39–43] Thus, we performed spotting assays on galactose plates containing high levels of manganese, demonstrating that exposure to manganese slightly aggravated αSyn-instigated cytotoxicity in concentrations that did not affect isogenic control cells (2 mM and 4 mM $Mn^{2+}$ ions, respectively; Figure 6a). Upon *PMR1* deletion, $Mn^{2+}$ was highly toxic (Figures 6a and b).

Furthermore, we generated strains that overexpress Pmr1p alone or in combination with αSyn and subjected these strains

to spotting and clonogenic survival assays on galactose plates with and without manganese. Notably, high levels of Pmr1p were *per se* toxic to yeast cells, and combined overexpression of Pmr1p and αSyn killed > 95% of all cells (Figures 6b and c). Complementation analyses in *PMR1*-deficient cells demonstrated that expression of Pmr1p could (i) restore αSyn cytotoxicity and (ii) supress manganese toxicity (Figures 6b and c).

To further investigate the contribution of $Ca^{2+}$ *versus* $Mn^{2+}$ transport activity of Pmr1p to the toxic consequences of αSyn expression, we additionally transfected WT and *PMR1*-deficient cells with two point mutants of Pmr1p that were defective for transport of either $Ca^{2+}$ ions (Pmr1p[D53A]) or $Mn^{2+}$ ions (Pmr1p[Q783A]).[36,44] Compared with native Pmr1p, the overexpression of these point mutants in the background of WT cells still was less toxic than that of native Pmr1p, and both mutated variants were slightly less effective in enforcing
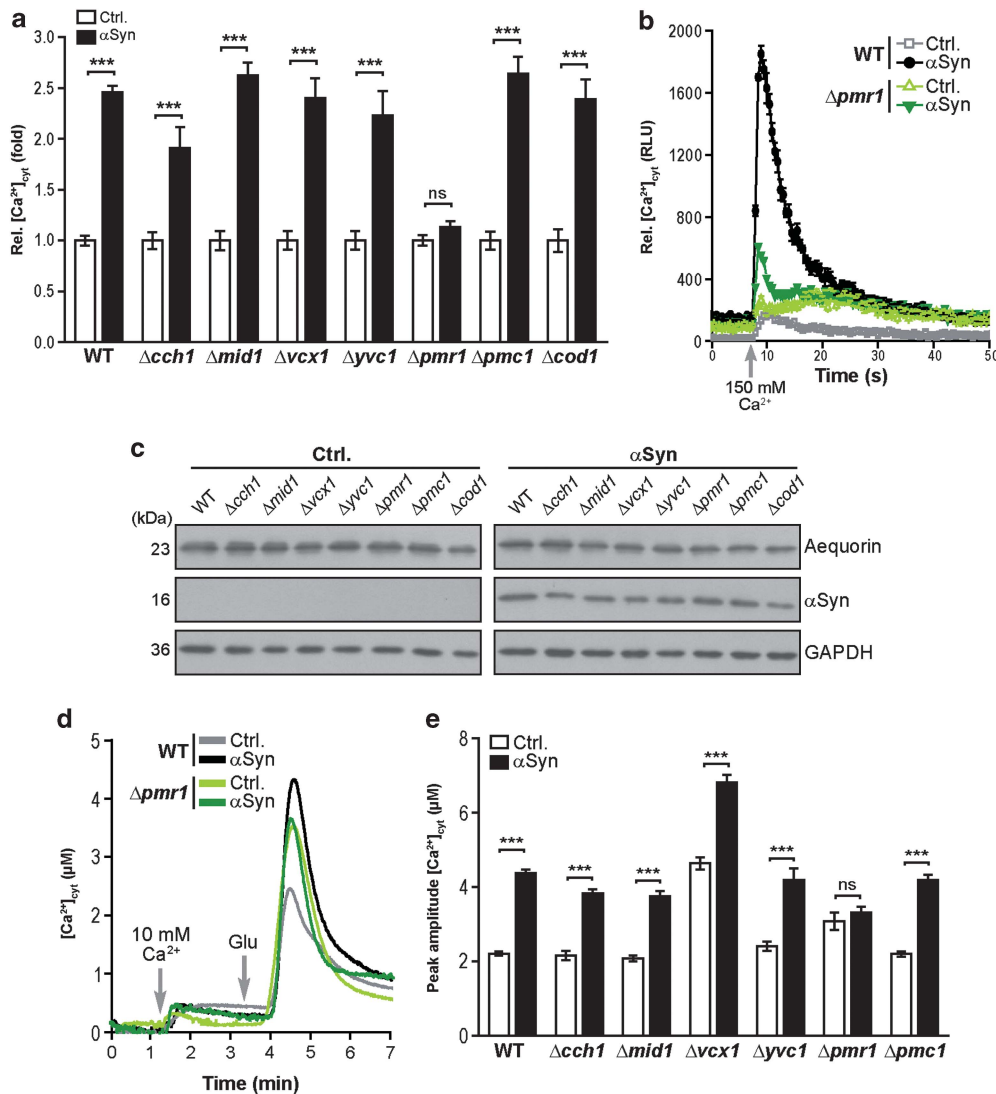
**Figure 5** Pmr1p is involved in αSyn-induced dysregulation of $Ca^{2+}$ homeostasis. (**a**) Aequorin-luminescence-based determination of basal cytosolic $Ca^{2+}$ levels in WT cells and indicated deletion mutants expressing αSyn for 20 h. Data was normalized to corresponding isogenic vector control. Mean ± S.E.M., $n = 12$; ***$P < 0.001$; NS, not significant. (**b**) Aequorin-equipped WT and Δ*pmr1* yeast cells expressing αSyn or harbouring the vector control were challenged with 150 mM $CaCl_2$ and transient $[Ca^{2+}]_{cyt}$ responses were observed for 50 s. Mean ± S.E.M., $n = 6$. (**c**) Western blot analysis of aequorin expression and αSyn expression in WT cells and indicated deletion mutants. Blots were probed with antibodies directed against aequorin, against FLAG-epitope to detect FLAG-tagged αSyn and against glyceraldehyd-3-phosphate dehydrogenase (GAPDH) as loading control. (**d**) Aequorin-equipped WT and Δ*pmr1* cells constitutively expressing αSyn (using the expression vector pGGE181) or harbouring the empty pGGE181 vector (Ctrl.) were starved for glucose, supplemented with low doses of $Ca^{2+}$ (10 mM) and subsequently challenged with 80 mM glucose. Transient $[Ca^{2+}]_{cyt}$ responses were monitored. Data represent average recordings, $n \geq 9$. (**e**) Maximum $[Ca^{2+}]_{cyt}$ peak amplitude after addition of 80 mM glucose as depicted in (**d**) in aequorin-equipped WT cells and indicated deletion mutants upon expression of αSyn. Mean ± S.E.M., $n \geq 9$; ***$P < 0.001$; NS, not significant

αSyn cytotoxicity as determined in spotting assays and survival plating on galactose plates with and without addition of $Mn^{2+}$ (Figures 7a and b). Conducting the same experiments in *PMR1*-deleted cells demonstrated that native Pmr1p and Pmr1p[Q783A], which displays a selective loss of $Mn^{2+}$ transport, both efficiently reinstated αSyn toxicity, whereas the Pmr1p[D53A] variant deficient in $Ca^{2+}$ transport partly lost this ability (Figures 7a and b). Native Pmr1p as well as Pmr1p[D53A] expectedly suppressed manganese toxicity of *PMR1*-deficient cells, whereas Pmr1p[Q783A] did not (Figures 7a and b). Expression of the Pmr1p variants and αSyn was confirmed in all strains (Figure 7c). These data indicate that

the $Ca^{2+}$ transport activity of Pmr1p – rather than that of $Mn^{2+}$ – contributes to αSyn-induced cell killing.

**αSyn neurotoxicity in nematodes and flies requires PMR1.** To test and challenge our finding *in vivo*, we analysed the effects of *PMR1* depletion on αSyn neurotoxicity in the nematode *Caenorhabditis elegans* and in the fruit fly *Drosophila melanogaster.* Nematodes expressing human αSyn directed by the dopamine transporter (*dat-1*) promoter were examined for survival of dopaminergic neurons. In WT nematodes, expression of αSyn resulted in the death of ∼40% of the dopaminergic neurons, while only ∼20% died
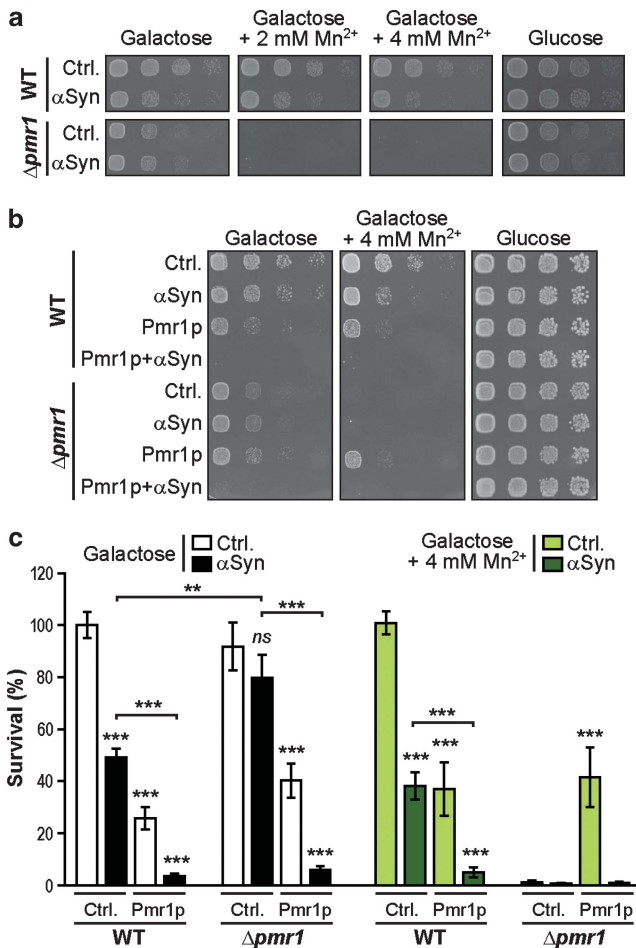
**Figure 6** Expression of Pmr1p restores αSyn cytotoxicity and supresses manganese toxicity of *PMR1*-deficient cells. (a) Spotting assays of WT and Δ*pmr1* yeast cells expressing αSyn or harbouring the vector control. Cells were grown for 24 h in galactose media and spotted in fivefold serial dilutions onto glucose (αSyn expression repressed) and galactose (αSyn expression induced) agar plates supplemented or not with 2 mM or 4 mM $Mn^{2+}$, respectively. (b) Spotting assays of WT and Δ*pmr1* yeast cells expressing either αSyn or Pmr1p alone or in combination or harbouring the corresponding vector controls. Cells were grown for 24 h in galactose media and spotted in fivefold serial dilutions onto glucose (Pmr1p and αSyn expression repressed) and galactose (Pmr1p and αSyn expression induced) agar plates supplemented or not with 4 mM $Mn^{2+}$. (c) Quantification of clonogenic survival of cells described in (b) after plating on galactose agar plates supplemented or not with 4 mM $Mn^{2+}$. Both Pmr1p as well as αSyn expression are driven by a galactose promoter. Mean ± S.E.M., $n = 8$–12; ***$P < 0.001$ and **$P < 0.01$; NS, not significant. Unless otherwise specified, asterisks indicate significances to similarly treated, isogenic control cells harbouring both empty vectors

in *PMR1*-deficient (*pmr-1(tm1840)*) animals (Figure 8a). Quantification of cytosolic $Ca^{2+}$ levels in αSyn-expressing dopaminergic neurons using the $Ca^{2+}$-sensitive fluorescent reporter protein GCaMP2.0[45] revealed that αSyn elevated the resting $[Ca^{2+}]_{cyt}$ in WT nematodes but not in *pmr-1(tm1840)* mutants (Figure 8b). In flies, the pan-neuronal *elav-GAL4*-driven expression of human αSyn significantly enhanced organismal death of male and female animals upon treatment with manganese. This effect was largely revised by RNA interference (RNAi)-mediated depletion of the Drosophila homologue of PMR1 (SPoCk) (Figures 8c and d). The absence of SPoCk did not affect the expression of

αSyn (Figure 8e). As αSyn is known to provoke locomotive deficits and the selective loss of tyrosine hydroxylase-positive dopaminergic neurons in Drosophila PD models,[16,46] we tested for a possible involvement of SPoCk in these neurotoxic consequences. The αSyn-induced decline in negative geotaxis (which drives flies to walk upwards after being tapped to the bottom of a vial) was prevented by depletion of SPoCk (Figure 8f). Furthermore, expression of αSyn caused a significant loss of dopaminergic neurons in defined clusters of the brain, and this effect was absent when SPoCk was depleted (Figures 8g and h). Thus, the toxic consequences of αSyn expression in yeast, nematodes and flies essentially involve the $Ca^{2+}$ ATPase PMR1.

## Discussion

Diverse $Ca^{2+}$ signals govern a myriad of vital functions, including mechanisms of fundamental neuronal biology such as synaptic transmission, plasticity, regulated neurite out-growth and synaptogenesis as well as pivotal generic processes like proliferation, transcription, differentiation and apoptosis. In particular, the mitochondrial cell death pathway is susceptible to elevated calcium concentrations.[47] Here, we establish that αSyn cytotoxicity is governed through sequentially occurring events, where the PMR1-dependent generation of a $[Ca^{2+}]_{cyt}$ increase precedes a burst of oxidative radicals that ultimately triggers cell death. In fact, the cytocidal effects of αSyn are reduced by treatment of cells with $Ca^{2+}$ chelators or by *PMR1* deletion as well as via treatment with the generic antioxidant NAC. Thus, whether αSyn is able to trigger elevated basal cytosolic $Ca^{2+}$ levels appears crucial for the subsequent cellular death. However, the transient $[Ca^{2+}]_{cyt}$ peaks following high external $Ca^{2+}$ or glucose pulses in αSyn-expressing cells, while remaining a good predictor of toxicity, are not fully stringent, as under specific conditions (e.g., upon deletion of *COD1* or *CCH1*), high $Ca^{2+}$ pulses were able to trigger massive transient $[Ca^{2+}]_{cyt}$ peaks without αSyn expression (Figure 5 and Supplementary Figure S3). The prominent role of $Ca^{2+}$ in αSyn-triggered cell death predicts that cellular $Ca^{2+}$ sensing/signalling mechanisms may modulate the detrimental effects of αSyn expression. In fact, disruption of calcineurin signalling results in exacerbated toxicity, suggesting a compensatory mechanism based on the recognition of abnormal $Ca^{2+}$ levels that partly counteracts the toxic consequences of αSyn. Cellular survival depends on tightly controlled $Ca^{2+}$ fluxes between cellular organelles as well as across the plasma membrane. Impaired $Ca^{2+}$ homeostasis and dysfunctional $Ca^{2+}$ signalling are implicated in a broad variety of neurodegenerative diseases besides PD, including Alzheimer's disease, Huntington's disease, Glaucoma, Amyotrophic Lateral Sclerosis, Epilepsy and even the psychiatric disorder Schizophrenia.[48] Upon $Ca^{2+}$ overload, mitochondria readily sequester and accumulate $Ca^{2+}$, which leads to enhanced production of ROS, and subsequently to dissipation of mitochondrial transmembrane potential, opening of the mitochondrial permeability transition pore and cellular demise.[47] For αSyn-induced cell death in particular, where the lethal role of mitochondria has been clearly established,[14,49–51] the molecular axis of toxicity might therefore converge in this organelle.
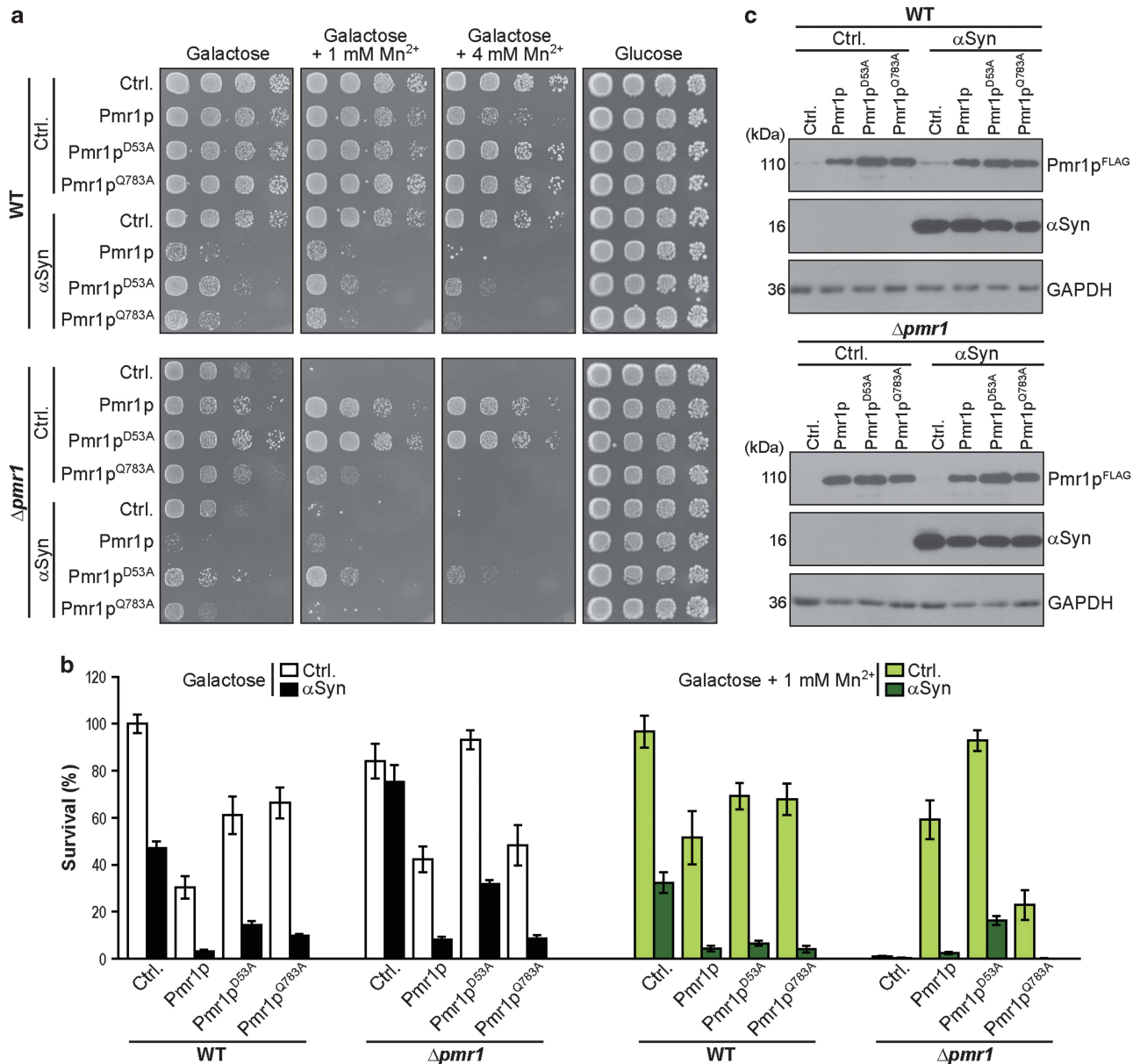
**Figure 7** $Ca^{2+}$ rather than $Mn^{2+}$ transport activity of Pmr1p contributes to αSyn toxicity. (**a**) Spotting assays of WT and Δ*pmr1* yeast cells expressing either Pmr1p or the point mutants Pmr1p$^{D53A}$ and Pmr1p$^{Q783A}$ alone or in combination with αSyn. Cells were grown for 24 h in galactose media and spotted in fivefold serial dilutions onto glucose (Pmr1p and αSyn expression repressed) and galactose (Pmr1p and αSyn expression induced) plates supplemented or not with 1 mM and 4 mM $Mn^{2+}$. (**b**) Cells described in (**a**) were subjected to clonogenic survival plating on galactose plates supplemented or not with 1 mM $Mn^{2+}$. Survival has been normalized to WT cells harbouring both empty vectors plated on galactose plates without manganese. Mean ± S.E.M., $n = 12–16$. (**c**) Western blot analysis of Pmr1p, Pmr1p$^{D53A}$ and Pmr1p$^{Q783A}$ overexpression as well as of αSyn expression in WT and Δ*pmr1* yeast cells. Blots were probed with antibodies directed against FLAG-epitope to detect FLAG-tagged Pmr1p variants and αSyn and against glyceraldehyd-3-phosphate dehydrogenase (GAPDH) as loading control

Our findings establish Pmr1p as a conserved mediator of αSyn cytotoxicity in yeast, nematodes and flies and indicate a toxic role for $Ca^{2+}$ in the pathology of PD. Enhancement of cytosolic calcium levels upon αSyn expression seems crucial for subsequent toxicity, a deadly road that requires PMR1.

**Experimental Procedures**
***Saccharomyces cerevisiae* strains, plasmids and media.**
Experiments were carried out in BY4741 (MATa *his3Δ1 leu2Δ0 met15Δ0 ura3Δ0*) and corresponding null mutants Δ*pmr1*, Δ*pmc1*, Δ*cch1*, Δ*mid1*, Δ*cod1*, Δ*vcx1*, Δ*yvc1*, Δ*cnb1*, Δ*cna1*, Δ*cna2*, Δ*crz1*, Δ*cmk1* and Δ*cmk2* as well as in

BY4741 harbouring endogenously GFP-tagged PMR1 (Euroscarf, Frankfurt, Germany). Strains were grown on SC medium containing 0.17% yeast nitrogen base (Difco, BD Biosciences, Schwechat, Austria), 0.5% $(NH_4)_2SO_4$ and 30 mg/l of all amino acids (except 80 mg/l histidine and 200 mg/l leucine), 30 mg/l adenine and 320 mg/l uracil with 2% glucose (SCD) or 2% galactose (SCG). Previously described αSyn-constructs in pESC-His (galactose promoter) or pUG23-His (methionine-repressible promoter)[14] or pGGE181 (constitutive promoter)[17] were deployed. To monitor cytosolic $Ca^{2+}$ levels, strains were transformed with the pYX212 vector encoding cytosolic aequorin (pYX212-cytAEQ) (kind gift from E. Martegani, Department of Biotechnology and Biosciences, University of Milano-Bicocca, Milan, Italy). To construct a conditional *PMR1* mutant, the promoter region of *PMR1* has been replaced by a tetO promoter (which prevents gene
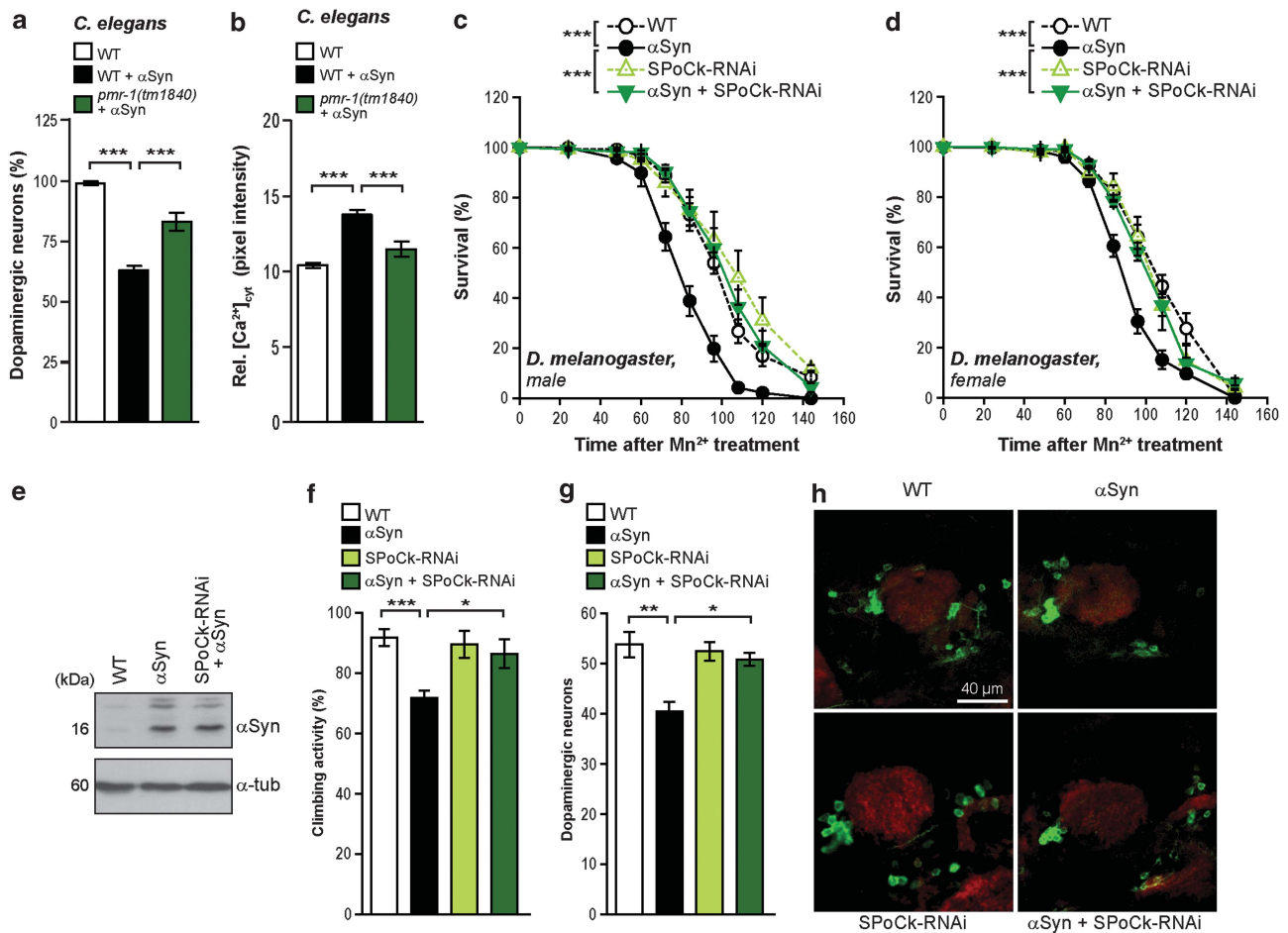
**Figure 8** PMR1 is critical for αSyn neurotoxicity in nematodes and flies. (**a**) Survival of *C. elegans* dopaminergic neurons in WT or PMR-1-deficient (*pmr-1(tm1840)*) animals expressing GFP and α-Syn. Mean ± S.E.M., $n > 250$ individual animals; ***$P < 0.001$. (**b**) Fluorescence-based quantification of cytoplasmic $Ca^{2+}$ levels in WT or PMR-1-deficient (*pmr-1(tm1840)*) nematodes expressing the $Ca^{2+}$ indicator GCaMP2.0 and α-Syn. Mean ± S.E.M., $n > 150$ dopaminergic neurons. ***$P < 0.001$. (**c** and **d**) Survival of male (**c**) and female (**d**) WT flies and of flies either expressing human αSyn or an RNAi depleting SPoCk (the Drosophila homologue of PMR1) or both (driven by *elav-GAL4*) upon supplementation of food (10% sucrose) with 20 mM $Mn^{2+}$. Means ± S.E.M., $n = 12$–20 with 35–40 flies per experiment; ***$P < 0.001$. (**e**) Immunoblot analysis of brain lysates obtained from flies expressing human αSyn driven by *elav-GAL4* with or without co-expression of an RNAi-depleting SPoCk using antibodies directed against human αSyn or Drosophila α-tubulin as loading control. (**f**) Climbing activity of female flies described in (**d**) after 24 h of $Mn^{2+}$ treatment. Means ± S.E.M., $n = 6$–10 with 8 flies per experiment; ***$P < 0.001$ and *$P < 0.05$. (**g** and **h**) Total count of tyrosine hydroxylase (TH)-immunoreactive dopaminergic neurons (**g**) in the DM, PM and DL1 brain clusters of female flies expressing αSyn alone or in combination with an RNAi-depleting SPoCk after treatment with $Mn^{2+}$ for 96 h. Representative confocal microscopy images of dissected brains immunostained for TH and for Bruchpilot (BRP[Nc82]) to visualize brain structure are shown in (**h**). Neuronal counts were quantified by inspection of the individual planes of the z-stack. Means ± S.E.M., $n = 5$–10; **$P < 0.01$ and *$P < 0.05$

expression upon addition of $\geq 10\,\mu g/ml$ doxycycline) following the protocol described by Yen *et al.*[28] Briefly, the KanMX-tetO₇ cassette has been amplified using pCM325 as template and the following primers: 5′-CAT TTT GTT ACA TCA AGA CAA GAT TCT CTA TTT AAA GAA GTA CGT ACG CTG CAG GTC GAC GG-3′ (forward) and 5′-AAT TAT CTT ATC TTT TAC TTA CAC TTA AGC TTA CGT CTG TGC TGG CAT AGG CCA CTA GTG GAT CTG-3′ (reverse). The amplified cassette has been integrated into the parental strain CML476 via homologous recombination.[28] To generate SOD1 and SOD2 constructs, inserts were amplified by PCR with primers 5′-ATC TGA ATT CAT GGT TCA AGC AGT CGC AG-3′ and 5′-ATC TAT CGA TGT TGG TTA GAC CAA TGA CAC C-3′ for SOD1 and 5′-ATC TGA ATT CAT GTT CGC GAA AAC AGC AGC-3′ and 5′-ATC TAT CGA TGA TCT TGC CAG CAT CGA ATC TTC-3′ for SOD2, cut with EcoRI and ClaI (Fermentas, Thermo Scientific, Vienna, Austria) and ligated into pUG35-Ura.[52] To generate PMR1 and the two point mutants PMR1[D53A] and PMR1[Q783A] in pESC-Ura (Stratagene, Agilent Technologies, Vienna, Austria), previously described plasmids coding for Pmr1p or respective point mutants were used as templates[36,44] (kind gift of R. Rao, Johns Hopkins University, Baltimore, Maryland,

USA). Inserts were amplified by PCR with the primers 5′-ATC TGC GGC CGC ATG AGT GAC AAT CCA TTT AAT GC-3′ and 5′-ATC TAC TAG TGT AAC ATT TGA GAA ATA CGT TGA GTC-3′, cut with NotI and Spel (Fermentas) and ligated into pESC-Ura.

**Analysis of *S. cerevisiae* survival, oxidative stress and apoptotic and necrotic changes.** To determine survival, oxidative stress, phosphatidylserine externalization and loss of membrane integrity upon expression of αSyn, cells from overnight cultures were inoculated in SCD to $OD_{600}$ 0.1, grown to midlog phase and shifted to SCG for induction of αSyn expression. Clonogenic survival plating was performed as previously described.[53,54] Briefly, a CASY cell counter (Schärfe System, Reutlingen, Germany) was used to measure the cell counts and 500 cells were either plated on full-media YEPD (1% yeast extract, 2% Bacto peptone, 4% glucose; Difco) agar plates (to repress further galactose-driven expression of αSyn and/or Pmr1p and point mutants) or on selective galactose agar plates (to induce expression of αSyn and/or Pmr1p) supplemented or not with 1 mM, 2 mM or 4 mM $MnCl_2$ as indicated. Colony-forming units were quantified

after 2 days (YEPD plates) or 3 days (galactose plates) of growth using a Scanalyser Colony Counter (LemnaTec, Wuerselen, Germany). To measure the level of cellular oxidative stress, cultures were subjected to DHE staining at indicated time points, followed by quantification using a fluorescence reader or flow cytometry as previously described.[55] Externalization of phosphatidylserine and loss of membrane integrity was quantified after 48 h of αSyn expression using Annexin V/propidium iodide co-staining as previously described.[55] For quantifications using flow cytometry (FACSAria, BD Biosciences, Schwechat, Austria), 30 000 cells were evaluated and analysed with BD FACSDiva software. Same cells were visualized via epifluorescence microscopy on a Zeiss Axioskop microscope (Zeiss, Vienna, Austria). Notably, at least four different clones were tested after plasmid transformation to rule out clonogenic variations. For experiments with the $Ca^{2+}$ chelators ethylene glycol tetraacetic acid and BAPTA-AM (Sigma, Vienna, Austria) and the antioxidant NAC (Sigma), cultures were either grown for 7 h after the shift on SCG for induction of αSyn expression and then supplemented with 2 mM ethylene glycol tetraacetic acid or 380 $\mu$M BAPTA-AM or treated with 20 mM and 30 mM NAC directly after the shift. For spotting assays, cells were grown in SCG for 24 h, adjusted to $5 \cdot 10^6$ cells/ml and spotted in fivefold serial dilutions onto glucose (expression repressed) and galactose (expression induced) agar plates supplemented or not with indicated concentrations of $Mn^{2+}$.

**S. cerevisiae cytosolic $Ca^{2+}$ measurement.** $[Ca^{2+}]_{cyt}$ were measured using yeast strains carrying the vector pYX212 encoding the bioluminescent protein aequorin under the control of a TPI promoter. For analysis of resting, basal $[Ca^{2+}]_{cyt}$ and of the cellular response to high doses of external $Ca^{2+}$, cells expressing αSyn under a galactose-inducible promoter (pESC-His) and equipped with pYX212-cytAEQ were inoculated in SCD to $OD_{600}$ 0.1, grown to midlog phase and shifted to SCG for induction of αSyn expression. At indicated time points, an equivalent of $6 \cdot 10^6$ cells was transferred into a 96 well plate and harvested by centrifugation. The pellets were resuspended in 200 $\mu$l SCG containing 4 $\mu$M coelenterazine and incubated for 1 h in the dark. To remove excess coelenterazine, the cells were washed once with fresh SCG and subsequently incubated for further 30 min. A LUMIstar Galaxy Luminometer (BMG Labtechnologies, Offenburg, Germany) was used to measure basal $[Ca^{2+}]_{cyt}$ as well as the response of $[Ca^{2+}]_{cyt}$ to external $Ca^{2+}$ shocks. The basal luminescence was measured per well in 0.5-s intervals for 25 s, whereas for kinetic luminescence measurements the signal was recorded for 70 s. In order to investigate the kinetics of the cellular response to an external $Ca^{2+}$ shock, a pump injected 40 $\mu$l of a 0.8 M $CaCl_2$ solution into each well. During all measurements, the plate was shaken and incubated at 28 °C. The luminescence signal was normalized to the $OD_{600}$ of each well and reported in relative luminescence units.

For analysis of glucose-induced transients after glucose starvation, yeast cells constitutively expressing αSyn (using the pGGE181 plasmid) transformed with pYX212-cytAEQ were grown in selective medium with 2% glucose. Cells taken from stationary-phase pre-cultures were used to inoculate a new culture. When cultures reached an $OD_{600}$ of ± 1.2, one $OD_{600}$ unit of cells was plated on concanavaline A-coated coverslips and incubated at 30 °C for 1 h. Cells were subsequently washed with 0.1 M 2-(N-morpholino) ethanesulphonic acid (MES)/Tris, pH 6.5, which is a nutrient-free buffer, and again incubated for 1 h at 30 °C with 0.1 M MES/Tris pH 6.5 supplemented with 5 $\mu$M wt coelenterazine (Promega, Mannheim, Germany). Excess of coelenterazine was removed by washing the cells three times with 0.1 M MES/Tris pH 6.5, and coverslips were mounted in a thermostated perfusion chamber (30 °C). Cells were initially perfused with 0.1 M MES/Tris pH 6.5, followed by 0.1 M MES/Tris pH 6.5 supplemented with 10 mM $CaCl_2$. Cells were then stimulated by addition of 80 mM glucose to induce a transient elevation of cytosolic $Ca^{2+}$ (TECC response) after glucose starvation.[56] At the end of the experiment, cells were lysed in a $Ca^{2+}$-rich hypotonic medium (10 mM $CaCl_2$ in $H_2O$) containing 0.5% Triton X-100. The recorded aequorin luminescence data were calibrated offline into cytosolic $Ca^{2+}$ values using the following algorithm $[Ca^{2+}]_{cyt} = ((L/L_{max})^{1/3} + [118(L/L_{max})^{1/3} - 1])/(7 \times 10^6 - [7 \times 10^6 (L/L_{max})^{1/3}])$, where $L$ is the luminescence intensity at any time point and $L_{max}$ is the integrated luminescence.[57]

**S. cerevisiae immunoblot analysis.** Immunoblot analysis of whole-cell extracts was performed as described.[53] Blots were probed with monoclonal antibodies against FLAG-epitope (Sigma), GFP (Sigma), glyceraldehyd-3-phosphate dehydrogenase (Sigma) and Aequorin (Abcam, Cambridge, UK) and the respective peroxidase-conjugated affinity-purified secondary antibodies (Sigma).

**Reverse transcription quantitative PCR.** To determine mRNA levels in yeast, total RNA was extracted from respective strains using Qiagen RNeasy kit (Qiagen, Hilden, Germany) with $5 \cdot 10^8$ cells per extraction. Contaminating DNA was removed by DNase I digestion using Qiagen RNase-Free DNase Set and RNA was cleaned up according to the Qiagen RNA cleanup and concentration protocol. RNA concentrations were determined with a NanoDrop Spectrophotometer (NanoDrop Technologies, Thermo Scientific, Vienna, Austria), and 100 ng were used for detection of mRNA levels of PMR1, CCH1 and MID1 and of actin mRNA (as endogenous housekeeping gene) via reverse transcription and quantitative PCR amplification using SensiMixTM SYBR one-Step Kit (Bioline, Wiener Neudorf, Austria) and a Corbett Research RG6000 PCR machine (Qiagen). The following primers were used at a concentration of 300 nM: PMR1 primers 5′-TCCTTAGCGGTTGCTGCTAT-3′ (forward) and 5′-TCCTTAGCGGTT GCTGCTAT-3′ (reverse), CCH1 primers 5′-GCTACGGTAATGGGTTCAGC-3′ (forward) and 5′-CGCCTTTTCCTCAATGGTAA-3′ (reverse), MID1 primers 5′-CGAACGCTACCTCCACGTAT-3′ (forward) and 5′-GGCCTTACATCCCACTG AAA-3′ (reverse) and actin primers 5′-GCCTTCTACGTTTCCATCCA-3′ (forward) and 5′-GGCCAAATGATTCTCAAAA-3′ (reverse), all amplifying a length between 150 and 160 bp. Cycling conditions were 10 min at 42 °C and 10 min at 95 °C, followed by 40 cycles of 15 s at 95 °C, 15 s at 60 °C and 15 s at 72 °C. The obtained mRNA levels were normalized to the mRNA levels of the actin housekeeping gene within the same sample.

**Statistical analysis.** A one-way ANOVA followed by a Bonferroni *post-hoc* test was used to calculate *P*-values. For survival of Drosophila, a two-way ANOVA with time and strain as independent factors followed by a Bonferroni *post-hoc* test was used.

**C. elegans strains and genetics.** We followed standard procedures for C. elegans strain maintenance.[58] Nematode-rearing temperature was kept at 20 °C, unless noted otherwise. The following strains were used in this study: N2: WT Bristol isolate (wt), *pmr-1(tm1840)*, *Ex[p$_{dat-1}$GCaMP2.0]*, *pmr-1(tm1840)X;Ex[p$_{dat-1}$GCaMP2.0]*, BZ555: *egIs1[p$_{dat-1}$GFP]*, UA44: *baIn11[p$_{dat-1}$α-Syn, p$_{dat-1}$GFP]*, *Ex[p$_{dat-1}$α-Syn, p$_{dat-1}$GCaMP2.0]*, *pmr-1(tm1840)X;Ex[p$_{dat-1}$α-Syn, p$_{dat-1}$GCaMP2.0]* and *pmr-1(tm1840)X;Ex[p$_{dat-1}$α-Syn, p$_{dat-1}$GFP]*. The BZ555 and UA44 strains were generously provided by Guy Caldwell (Department of Biological Sciences, The University of Alabama).

**C. elegans neurodegeneration analysis.** Seven-day-old animals were used for αSyn-induced neurodegeneration quantification. The four CEP dopaminergic neurons in the worm of the head were scored as described previously.[59] Experiments were repeated four times, and statistical analyses were performed using the GraphPad Prism software package (GraphPad Software, San Diego, USA). Analysis of variance (ANOVA) was used for comparisons of multiple groups of values (in both approaches of neurodegeneration analysis), followed by Bonferroni multiple-group comparison tests.

**C. elegans monitoring of cytosolic $Ca^{2+}$ levels.** For intracellular $Ca^{2+}$ monitoring experiments, transgenic animals expressing the $Ca^{2+}$ reporter GCaMP2.0[45] in dopaminergic neurons were examined under a Zeiss AxioImager Z2 epifluorescence microscope (Zeiss, Thessaloniki, Greece). The four CEP dopaminergic neurons in the worm of the head were imaged. Only neurons of very initial stages of degeneration (based on morphological features using DIC microscopy) were used for analysis, as the expression of GCaMP2.0 ceases during later stages of neurodegeneration. The emission intensity of GCaMP2.0 was calculated by using the ImageJ software (http://rsb.info.nih.gov/ij/).

**D. melanogaster strains, genetics and survival.** The line UAS-αSyn was obtained from the Bloomington Stock Centre (Indiana University, USA). The UAS-CG32451RNAi (SPoCk, the Drosophila homologue of PMR1) line (transformant 110379) was obtained from the Vienna Drosophila RNAi Centre (Vienna, Austria). Lines overexpressing αSyn were crossed with the RNAi line to create the following stable stocks of flies: UAS-CG32451RNAi/ UAS-CG32451RNAi; UAS-αSyn/UAS-αSyn. A chromosome III-linked elav-GAL4 enhancer trap line was used to drive expression. To determine survival upon challenge with manganese, 1–3-day-old flies (both sexes, kept separately) were incubated at 29 °C for 24 h and transferred into fresh vials with filter papers soaked with solution containing 10% sucrose and 20 mM $MnCl_2$. Filters were kept wet at all times and numbers of dead flies were recorded at indicated time points. Each

476

experiment was performed with 35–40 flies and repeated 12–20 times (as indicated in the respective figure legend).

### D. melanogaster determination of locomotive ability.

To determine climbing ability upon supplementation of food with 20 mM $Mn^{2+}$ ions for 24 h, eight female flies were placed into a vertical plastic tube with a diameter of 1.5 cm and gently tapped to the bottom. Flies reaching a specific mark (10 cm) within 10 sec were counted. Experiments were conducted in the dark (red light). Six trials of climbing were performed for each set of eight flies to determine the mean climbing activity per experiment, and at least six independent experiments were performed for each genotype.

### D. melanogaster immunostaining and immunoblotting.

Immunostaining was essentially performed as described before.[60] Brains were dissected in HL3 on ice, fixed in cold 4% PBS for 20 min and washed four times for 15 min in 0.3% PBT. After 1 h in PBT with 10% NGS at RT, brains were incubated for 2 days in PBT with 5% NGS containing primary antibodies against tyrosine hydroxylase (Millipore, Schwalbach, Germany) to detect dopaminergic neurons and against Bruchpilot (BRP[Nc82]) to visualize brain structure and then washed in PBT four times for 20 min. Subsequently, brains were incubated in PBT with 5% NGS, and the respective secondary antibodies labelled with FITC or Cy3 (Invitrogen, Darmstadt, Germany) for 1 day. Finally, brains were washed four times in PBT and transferred onto slides in Vectashield (Vector laboratories, Lörrach, Germany). Image acquisition was performed with a confocal microscope (TCS SP5, Leica Microsystems, Wetzlar, Germany) using the LCS AF software (Leica Microsystems). For immunoblot analysis, 20–30 fly heads were homogenized on ice in 50 μl 2% SDS with protease inhibitor cocktail (Roche Diagnostics, Mannheim, Germany). Equal volume of 2 × Lämmli was added, samples were incubated at 95 °C for 5 min and then kept at RT for 5 min before centrifugation for 5 min at 13 000 × g and subsequent SDS-PAGE analysis. Blots were probed with primary antibodies against α-tubulin (Abcam) and αSyn (Sigma) and respective secondary antibodies.

## Conflict of Interest

The authors declare no conflict of interest.

1. Spillantini MG, Schmidt ML, Lee VM, Trojanowski JQ, Jakes R, Goedert M. Alpha-synuclein in Lewy bodies. Nature 1997; 388: 839–840.
2. Kruger R, Kuhn W, Müller T, Woitalla D, Graeber M, Kösel S et al. Ala30Pro mutation in the gene encoding alpha-synuclein in Parkinson's disease. Nat.Genet 1998; 18: 106–108.
3. Singleton AB, Farrer M, Johnson J, Singleton A, Hague S, Kachergus J et al. alpha-Synuclein locus triplication causes Parkinson's disease. Science 2003; 302: 841.
4. Zarranz JJ, Alegre J, Gómez-Esteban JC, Lezcano E, Ros R, Ampuero I et al. The new mutation, E46K, of alpha-synuclein causes Parkinson and Lewy body dementia. Ann.Neurol. 2004; 55: 164–173.
5. Farrer M, Kachergus J, Forno L, Lincoln S, Wang DS, Hulihan M et al. Comparison of kindreds with parkinsonism and alpha-synuclein genomic multiplications. Ann. Neurol 2004; 55: 174–179.
6. Polymeropoulos MH, Lavedan C, Leroy E, Ide SE, Dehejia A, Dutra A et al. Mutation in the alpha-synuclein gene identified in families with Parkinson's disease. Science 1997; 276: 2045–2047.
7. Chan CS, Guzman JN, Ilijic E, Mercer JN, Rick C, Tkatch T et al. 'Rejuvenation' protects neurons in mouse models of Parkinson's disease. Nature 2007; 447: 1081–1086.
8. Cali T, Ottolini D, Brini M. Mitochondria, calcium, and endoplasmic reticulum stress in Parkinson's disease. Biofactors 2011; 37: 228–240.
9. Lowe R, Pountney DL, Jensen PH, Gai WP, Voelcker NH. Calcium(II) selectively induces alpha-synuclein annular oligomers via interaction with the C-terminal domain. Protein Sci 2004; 13: 3245–3252.
10. Adamczyk A, Strosznajder JB. Alpha-synuclein potentiates Ca2 + influx through voltage-dependent Ca2 + channels. Neuroreport 2006; 17: 1883–1886.
11. Hettiarachchi NT, Parker A, Dallas ML, Pennington K, Hung CC, Pearson HA et al. alpha-Synuclein modulation of Ca2 + signaling in human neuroblastoma (SH-SY5Y) cells. J Neurochem 2009; 111: 1192–1201.
12. Danzer KM, Haasen D, Karow AR, Moussaud S, Habeck M, Giese A et al. Different species of alpha-synuclein oligomers induce calcium influx and seeding. J Neurosci 2007; 27: 9220–9232.
13. Khurana V, Lindquist S. Modelling neurodegeneration in Saccharomyces cerevisiae: why cook with baker's yeast? Nat Rev Neurosci 2010; 11: 436–449.
14. Büttner S, Bitto A, Ring J, Augsten M, Zabrocki P, Eisenberg T et al. Functional mitochondria are required for alpha-synuclein toxicity in aging yeast. J Biol Chem 2008; 283: 7554–7560.
15. Outeiro TF, Lindquist S. Yeast cells provide insight into alpha-synuclein biology and pathobiology. Science 2003; 302: 1772–1775.
16. Cooper AA, Gitler AD, Cashikar A, Haynes CM, Hill KJ, Bhullar B et al. Alpha-synuclein blocks ER-Golgi traffic and Rab1 rescues neuron loss in Parkinson's models. Science 2006; 313: 324–328.
17. Zabrocki P, Bastiaens I, Delay C, Bammens T, Ghillebert R, Pellens K et al. Phosphorylation, lipid raft interaction and traffic of alpha-synuclein in a yeast model for Parkinson. Biochim Biophys Acta 2008; 1783: 1767–1780.
18. Ton V-K, Rao R. Functional expression of heterologous proteins in yeast: insights into Ca2 + signaling and Ca2 + -transporting ATPases. Am J Physiol Cell Physiol 2004; 287: C580–C589.
19. Cronin SR, Rao R, Hampton RY. Cod1p/Spf1p is a P-type ATPase involved in ER function and Ca2 + homeostasis. J Cell Biol 2002; 157: 1017–1028.
20. Cui J, Kaandorp JA, Sloot PMA, Lloyd CM, Filatov MV. Calcium homeostasis and signaling in yeast cells and cardiac myocytes. FEMS Yeast Res 2009; 9: 1137–1147.
21. Abou-Sleiman PM, Muqit MM, Wood NW. Expanding insights of mitochondrial dysfunction in Parkinson's disease. Nat Rev Neurosci 2006; 7: 207–219.
22. Jenner P. Oxidative stress in Parkinson's disease. Ann Neurol 2003; 53(Suppl 3): S26–S36; discussion S36-8., S26–S36.
23. Jomova K, Vondrakova D, Lawson M, Valko M. Metals, oxidative stress and neurodegenerative disorders. Mol Cell Biochem 2010; 345: 91–104.
24. Sun L, Gu L, Wang S, Yuan J, Yang H, Zhu J et al. N-acetylcysteine protects against apoptosis through modulation of group I metabotropic glutamate receptor activity. PLoS ONE 2012; 7: e32503.
25. Berman AE, Chan WY, Brennan AM, Reyes RC, Adler BL, Suh SW et al. N-acetylcysteine prevents loss of dopaminergic neurons in the EAAC1-/- mouse. Ann Neurol 2011; 69: 509–520.
26. Clark J, Clore EL, Zheng K, Adame A, Masliah E, Simon DK. Oral N-acetyl-cysteine attenuates loss of dopaminergic terminals in alpha-synuclein overexpressing mice. PLoS ONE 2010; 5: e12333.
27. Bagh MB, Maiti AK, Jana S, Banerjee K, Roy A, Chakrabarti S. Quinone and oxyradical scavenging properties of N-acetylcysteine prevent dopamine mediated inhibition of Na +, K + -ATPase and mitochondrial electron transport chain activity in rat brain: implications in the neuroprotective therapy of Parkinson's disease. Free Radic Res 2008; 42: 574–581.
28. Yen K, Gitsham P, Wishart J, Oliver SG, Zhang N. An improved tetO promoter replacement system for regulating the expression of yeast genes. Yeast 2003; 20: 1255–1262.
29. Bonilla M, Nastase KK, Cunningham KW. Essential role of calcineurin in response to endoplasmic reticulum stress. EMBO J 2002; 21: 2343–2353.
30. Miseta A, Fu L, Kellermayer R, Buckley J, Bedwell DM. The Golgi apparatus plays a significant role in the maintenance of Ca2 + homeostasis in the vps33Delta vacuolar biogenesis mutant of Saccharomyces cerevisiae. J Biol Chem 1999; 274: 5939–5947.
31. Martin DC, Kim H, Mackin NA, Maldonado-Báez L, Evangelista CC Jr, Beaudry VG et al. New regulators of a high affinity Ca2 + influx system revealed through a genome-wide screen in yeast. J Biol Chem 2011; 286: 10744–10754.
32. Locke EG, Bonilla M, Liang L, Takita Y, Cunningham KW. A homolog of voltage-gated Ca(2 + ) channels stimulated by depletion of secretory Ca(2 + ) in yeast. Mol Cell Biol 2000; 20: 6686–6694.
33. Dürr G, Strayle J, Plemper R, Elbs S, Klee SK, Catty P et al. The medial-Golgi ion pump Pmr1 supplies the yeast secretory pathway with Ca2 + and Mn2 + required for glycosylation, sorting, and endoplasmic reticulum-associated protein degradation. Mol Biol Cell 1998; 9: 1149–1162.
34. Cunningham KW. Acidic calcium stores of Saccharomyces cerevisiae. Cell Calcium 2011; 50: 129–138.
35. Ton V-K, Mandal D, Vahadji C, Rao R. Functional expression in yeast of the human secretory pathway Ca(2 + ), Mn(2 + )-ATPase defective in Hailey-Hailey disease. J Biol Chem 2002; 277: 6422–6427.
36. Mandal D, Woolf TB, Rao R. Manganese selectivity of pmr1, the yeast secretory pathway ion pump, is defined by residue gln783 in transmembrane segment 6. Residue Asp778 is essential for cation transport. J Biol Chem 2000; 275: 23933–23938.
37. Olanow CW. Manganese-induced parkinsonism and Parkinson's disease. Ann N Y Acad Sci 2004; 1012: 209–223.
38. Pal PK, Samii A, Calne DB. Manganese neurotoxicity: a review of clinical features, imaging and pathology. Neurotoxicology 1999; 20: 227–238.
39. Gitler AD, Chesi A, Geddie ML, Strathearn KE, Hamamichi S, Hill KJ et al. Alpha-synuclein is part of a diverse and highly conserved interaction network that includes PARK9 and manganese toxicity. Nat Genet 2009; 41: 308–315.

40. Covy JP, Giasson BI. α-Synuclein, leucine-rich repeat kinase-2, and manganese in the pathogenesis of Parkinson disease. *Neurotoxicology* 2011; **32**: 622–629.
41. Covy JP, Waxman EA, Giasson BI. Characterization of cellular protective effects of ATP13A2/PARK9 expression and alterations resulting from pathogenic mutants. *J Neurosci Res* 2012; **90**: 2306–2316.
42. Tan J, Zhang T, Jiang L, Chi J, Hu D, Pan Q *et al.* Regulation of intracellular manganese homeostasis by Kufor-Rakeb syndrome-associated ATP13A2 protein. *J Biol Chem* 2011; **286**: 29654–29662.
43. Settivari R, Levora J, Nass R. The divalent metal transporter homologues SMF-1/2 mediate dopamine neuron sensitivity in caenorhabditis elegans models of manganism and parkinson disease. *J Biol Chem* 2009; **284**: 35758–35768.
44. Wei Y, Marchi V, Wang R, Rao R. An N-terminal EF hand-like motif modulates ion transport by Pmr1, the yeast Golgi Ca(2 + )/Mn(2 + )-ATPase. *Biochemistry* 1999; **38**: 14534–14541.
45. Nakai J, Ohkura M, Imoto K. A high signal-to-noise Ca(2 + ) probe composed of a single green fluorescent protein. *Nat Biotechnol* 2001; **19**: 137–141.
46. Feany MB, Bender WW. A Drosophila model of Parkinson's disease. *Nature* 2000; **404**: 394–398.
47. Orrenius S, Zhivotovsky B, Nicotera P. Regulation of cell death: the calcium-apoptosis link. *Nat Rev Mol Cell Biol* 2003; **4**: 552–565.
48. Wojda U, Salinska E, Kuznicki J. Calcium ions in neuronal degeneration. *IUBMB Life* 2008; **60**: 575–590.
49. Schapira AHV, Gegg M. Mitochondrial contribution to Parkinson's disease pathogenesis. *Parkinsons Dis* 2011; **2011**: 159160.
50. Protter D, Lang C, Cooper AA. αSynuclein and mitochondrial dysfunction: a pathogenic partnership in Parkinson's disease? *Parkinsons Dis* 2012; **2012**: 829207.
51. Kamp F, Exner N, Lutz AK, Wender N, Hegermann J, Brunner B *et al.* Inhibition of mitochondrial fusion by α-synuclein is rescued by PINK1, Parkin and DJ-1. *EMBO J* 2010; **29**: 3571–3589.
52. Niedenthal RK, Riles L, Johnston M, Hegemann JH. Green fluorescent protein as a marker for gene expression and subcellular localization in budding yeast. *Yeast* 1996; **12**: 773–786.
53. Madeo F, Herker E, Maldener C, Wissing S, Lächelt S, Herlan M *et al.* A caspase-related protease regulates apoptosis in yeast. *Mol Cell* 2002; **9**: 911–917.
54. Herker E, Jungwirth H, Lehmann KA, Maldener C, Fröhlich KU, Wissing S *et al.* Chronological aging leads to apoptosis in yeast. *J Cell Biol* 2004; **164**: 501–507.
55. Büttner S, Eisenberg T, Carmona-Gutierrez D, Ruli D, Knauer H, Ruckenstuhl C *et al.* Endonuclease G regulates budding yeast life and death. *Mol Cell* 2007; **25**: 233–246.
56. Kellermayer R, Szigeti R, Kellermayer M, Miseta A. The intracellular dissipation of cytosolic calcium following glucose re-addition to carbohydrate depleted *Saccharomyces cerevisiae*. *FEBS Lett* 2004; **571**: 55–60.
57. Gupta SS, Ton VK, Beaudry V, Rulli S, Cunningham K, Rao R. Antifungal activity of amiodarone is mediated by disruption of calcium homeostasis. *J Biol Chem* 2003; **278**: 28831–28839.
58. Brenner S. The genetics of Caenorhabditis elegans. *Genetics* 1974; **77**: 71–94.
59. Qiao L, Hamamichi S, Caldwell KA, Caldwell GA, Yacoubian TA, Wilson S *et al.* Lysosomal enzyme cathepsin D protects against alpha-synuclein aggregation and toxicity. *Mol Brain* 2008; **1**: 17.
60. Owald D, Fouquet W, Schmidt M, Wichmann C, Mertel S, Depner H *et al.* A Syd-1 homologue regulates pre- and postsynaptic maturation in Drosophila. *J Cell Biol* 2010; **188**: 565–579.

Supplementary Information accompanies the paper on Cell Death and Differentiation website (http://www.nature.com/cdd)